

Repeated Anaerobic Microbial Redox Cycling of Iron^{∇†}

Aaron J. Coby,^{1‡} Flynn Picardal,² Evgenya Shelobolina,¹ Huifang Xu,¹ and Eric E. Roden^{1*}

Department of Geoscience, University of Wisconsin, Madison, Wisconsin 53706,¹ and School of Public and Environmental Affairs, Indiana University, Bloomington, Indiana 47405²

Received 7 February 2011/Accepted 28 June 2011

Some nitrate- and Fe(III)-reducing microorganisms are capable of oxidizing Fe(II) with nitrate as the electron acceptor. This enzymatic pathway may facilitate the development of anaerobic microbial communities that take advantage of the energy available during Fe-N redox oscillations. We examined this phenomenon in synthetic Fe(III) oxide (nanocrystalline goethite) suspensions inoculated with microflora from freshwater river floodplain sediments. Nitrate and acetate were added at alternate intervals in order to induce repeated cycles of microbial Fe(III) reduction and nitrate-dependent Fe(II) oxidation. Addition of nitrate to reduced, acetate-depleted suspensions resulted in rapid Fe(II) oxidation and accumulation of ammonium. High-resolution transmission electron microscopic analysis of material from Fe redox cycling reactors showed amorphous coatings on the goethite nanocrystals that were not observed in reactors operated under strictly nitrate- or Fe(III)-reducing conditions. Microbial communities associated with N and Fe redox metabolism were assessed using a combination of most-probable-number enumerations and 16S rRNA gene analysis. The nitrate-reducing and Fe(III)-reducing cultures were dominated by denitrifying *Betaproteobacteria* (e.g., *Dechloromonas*) and Fe(III)-reducing *Deltaproteobacteria* (*Geobacter*), respectively; these same taxa were dominant in the Fe cycling cultures. The combined chemical and microbiological data suggest that both *Geobacter* and various *Betaproteobacteria* participated in nitrate-dependent Fe(II) oxidation in the cycling cultures. Microbially driven Fe-N redox cycling may have important consequences for both the fate of N and the abundance and reactivity of Fe(III) oxides in sediments.

Oxygen, nitrate, and Mn(IV) oxides are the primary oxidants for Fe(II) in natural systems. Fe(II) is subject to spontaneous chemical oxidation by oxygen and Mn(IV) oxides at circumneutral pH (16, 31, 33, 36). In contrast, the abiotic reaction of Fe(II) with nitrate is negligible under the temperature and aqueous geochemical conditions typical of natural soil and sedimentary environments (58). Although the presence of nitrate-reducing, Fe(II)-oxidizing organisms has been documented in a wide variety of environments (5, 13, 25, 28, 37, 40, 49, 51, 52), little is known about the quantitative coupling of Fe and N redox cycles in sediments. In particular, virtually nothing is known about Fe-N redox cycling in sediments subject to spatial or temporal shifts in redox conditions.

The input of oxidants compared to utilizable organic carbon controls the predominant terminal electron-accepting pathway (TEAP) in a given soil or sediment horizon. Where the fluxes of oxidants and organic carbon are relatively constant, sequential consumption of electron acceptors leads to the formation of stable redox gradients (3, 20). Many subsurface environments that are very active hydrologically and which support a diverse microflora (11), e.g., local-flow groundwater systems (12), however, are characterized by large fluctuations in chemical conditions. Redox fluctuations in such environments are likely to have a critical impact on Fe species content and

thereby strongly influence the behavior of natural and contaminant compounds whose behavior is linked to Fe redox cycling.

Nitrate-dependent Fe(II) oxidation enhances the potential for coupled Fe-N redox interactions in sediments and may be associated with the development of microbial populations specifically adapted to take advantage of the energy available during redox oscillations (53, 60). Transient redox fluctuations can also have a significant impact on Fe(III) oxide mineralogy (15), although the cumulative effects of such fluctuations are not well known (54). In this paper we present the results of batch experiments designed to explore geochemical and microbiological phenomena associated with anaerobic Fe-N redox cycling in reaction systems experiencing repeated fluctuations in organic carbon (acetate) and nitrate loading.

MATERIALS AND METHODS

Culture medium. O₂-free, N₂-bubbled, 1,4-piperazinediethanesulfonic acid (PIPES)-buffered (10 mM, pH 6.8) artificial groundwater (AGW) medium (60) containing (per liter) 5.5 g (62 mmol) goethite (α -FeOOH) synthesized by air oxidation of FeCl₂ · 2H₂O in NaHCO₃ buffer (44) was used in all experiments. This goethite corresponds to the “high-surface goethite” (surface area, ca. 150 m² g⁻¹; average particle size, 15 to 30 nm) discussed in reference 43. Previous studies have demonstrated that the abundance of amorphous impurities (e.g., ferrihydrite) is very small in this material (42), and transmission electron microscopy (TEM) analysis verified the absence of amorphous phases in the starting material (see below). Goethite rather than ferrihydrite was used in these experiments because ferrihydrite typically undergoes major phase transformations during microbial reduction (61), which could have complicated assessment of the potential for nitrate-driven Fe redox cycling.

Incubation experiments. Three experiments were conducted in duplicate. System 1 (nitrate reducing) was amended with limiting acetate (2.0 mM) relative to nitrate (2.2 mM). System 2 [Fe(III) reducing] was amended with 2.0 mM acetate only. System 3 (Fe redox cycling) was initially amended with 2.1 mM acetate and 1.0 mM nitrate, and upon depletion, subsequent additions of either acetate or nitrate were made to induce Fe redox cycling. The system 1 and system 2 incubations lasted for only a few weeks, as nitrate reduction and Fe(III) reduc-

* Corresponding author. Mailing address: Department of Geoscience, 1215 W. Dayton St., Madison, WI 53706. Phone: (608) 890-0724. Fax: (608) 262-0693. E-mail: eroden@geology.wisc.edu.

‡ Present address: Saint Martin's University, 5300 Pacific Ave., S.E., Lacey, WA 98503.

† Supplemental material for this article may be found at <http://aem.asm.org/>.

∇ Published ahead of print on 8 July 2011.

tion ceased after ca. 1 and 2 weeks, respectively. In contrast, the Fe redox cycling experiment went on much longer (140 days) in order to assess the potential for repeated coupled Fe/N redox metabolism.

Acetate and nitrate were added from sterile, anaerobic stock solutions. Each reactor was inoculated with 5 ml of fresh surface sediment (0 to 2 cm) collected from near the banks of the Wisconsin River, three miles west of Portage, WI (close to site S3 described by Forshay and Stanley [19]). The sediment contained approximately equal concentrations (ca. 20 mmol liter⁻¹) of 0.5 M HCl-extractable Fe(II) and Fe(III), indicating active Fe(III) reduction (30). Although sediment pore fluids were depleted in nitrate, the section of the Wisconsin River from which the inoculum was obtained contains ca. 0.1 mM nitrate, and floodplain sediments are strong sinks for nitrate (19).

Samples for determination of Fe(II) (aqueous and solid associated), nitrate, ammonium, and acetate analyses were taken immediately after bottles were inoculated and then every 2 to 5 days for up to 135 days. Between sampling periods, the bottles were stored in the dark at room temperature without shaking. The contents of the bottles were resuspended before taking 1.5-ml samples with an N₂-flushed syringe. The aqueous phase was separated by centrifugation (12,000 × g for 10 min) in an anaerobic chamber (95% N₂, 5% H₂). For microbial community analysis, 5-ml samples were removed at the beginnings and ends of the experiments and stored anaerobically at -20°C.

Enumeration, enrichment, and isolation. At the ends of the incubation experiments, bacterial populations were enumerated as CFU using an anaerobic roll-tube method (26). Ten-fold serial dilutions were made in anaerobic AGW; 1-ml subsamples from each dilution were introduced into duplicate tubes containing 7 ml of sterile, anaerobic AGW liquefied agar (1.5% at 50°C) with the appropriate electron donor/acceptor. Enumerations were made for (i) nitrate-reducing (5 mM nitrate, 10 mM acetate), (ii) mixotrophic nitrate-reducing, Fe(II)-oxidizing (0.5 mM acetate, 5 mM nitrate, 5 mM FeCl₂ · 2H₂O) [referred to here as Fe(II)], (iii) autotrophic nitrate-reducing, Fe(II)-oxidizing [5 mM nitrate, 5 mM Fe(II)], and (iv) Fe(III)-reducing [80 mmol liter⁻¹ synthetic amorphous Fe(III) oxide (29), 10 mM acetate] organisms. The contents of the inoculated tubes were mixed, and the tubes were spun rapidly on a Belloco tube spinner until the agar had cooled on the sides of the culture tube. After 4 to 5 weeks of incubation in the dark at room temperature, colonies formed on the sides of the tubes were enumerated and the CFU per ml of inoculum were calculated.

Acetate-utilizing nitrate- and Fe(III)-reducing bacteria were enriched in AGW medium with 5 mM acetate, 50 mg liter⁻¹ yeast extract (YE), and either 5 mM nitrate or 100 mmol synthetic goethite per liter. Nitrate reducers were isolated following sequential transfers of anaerobic enrichment cultures on AGW medium with 5 mM nitrate and 5 mM acetate. Single colonies from a highly enriched culture were selected from medium solidified with 1.5% Noble agar. Nitrate-reducing isolates were identified phylogenetically based on their 16S rRNA gene sequences as described below.

Stable goethite-reducing cultures were obtained from all three systems. Roll-tube isolation procedures with either (i) acetate and amorphous Fe(III) oxide or (ii) a combined mixture (referred to as "nfa mix") of electron donors and acceptors (5 mM pyruvate, 10 mM acetate, 5 mM nitrate, 10 mM fumarate, 25 mg liter⁻¹ YE) were applied to attempt isolation of dissimilatory iron-reducing bacteria (DIRB) for each system. Pure cultures so obtained were grown in nfa mix and transferred to medium containing 10 mM Fe(III)-nitritotriacetic acid [Fe(III)-NTA] to test for Fe(III) reduction activity. Some cultures were also tested for the ability to utilize fumarate (10 mM) as an electron acceptor for anaerobic growth. Nearly-full-length 16S rRNA gene sequences were obtained for each isolate as described below.

16S rRNA gene analysis. Subsamples removed from duplicate reactors were pooled prior to extraction of genomic DNA using the MoBio UltraClean soil DNA kit. Materials from the initial (time zero) samples were similarly pooled and extracted. Purified DNA was amplified using the universal bacterial primer set GM3F-GM4R (35), resulting in a PCR product length of approximately 1.5 kb. DNA extracts from acetate/goethite enrichment cultures were amplified using 8F and 907R primers. PCR products were purified using a MinElute PCR purification kit. The purified product was ligated using a Promega pGEM-T Easy Vector System kit, transformed into competent *Escherichia coli* cells, and plated on LB agar containing 100 μg ml⁻¹ ampicillin and X-Gal (5-bromo-4-chloro-3-indolyl-β-D-galactopyranoside). Transformants were incubated at 37°C overnight, and colonies with recombinant vectors were selected. Recombinant vectors were grown overnight in LB broth at 37°C. Plasmids were isolated using a Promega Wizard DNA purification kit and sequenced at the University of Wisconsin Biotechnology Center.

DNA extracts from several samples were sent to Microbial Insights, Inc., for denaturing gradient gel electrophoresis (DGGE) analysis of 16S rRNA genes as

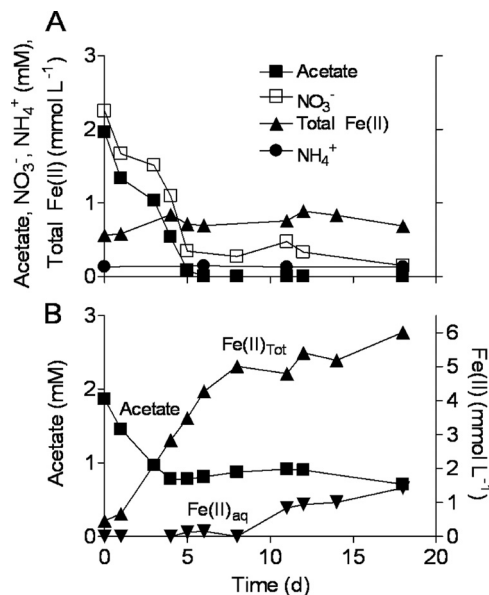


FIG. 1. Nitrate and Fe(III) reduction coupled to oxidation of acetate in batch suspensions of synthetic goethite containing excess nitrate (system 1; nitrate-reducing cultures) (A) or lacking nitrate [system 2; Fe(III)-reducing cultures] (B). Data represent means for duplicate cultures.

previously described (10). Prominent bands were excised, and the DNA contained in them was reamplified and sequenced.

Sequence data from the clone library and DGGE analyses were manually edited using the BioEdit program (version 7.0.5.3) (24) to remove vector sequences and eliminate poorly resolved regions. Whenever possible, edited sequences were assigned genus-level taxonomic affiliation by way of BLAST (1) searches. A value of 95% similarity was used as a cutoff for assignment of genus-level affiliation (21). In a few cases, only family-level affiliations could be assigned. In one instance, a collection of five diverse *Alphaproteobacteria* from the Fe(III)-reducing cultures were grouped together as "other *Alphaproteobacteria*."

Analytical methods. Acetate, nitrate, and nitrite concentrations were measured using a Dionex 1000 ion chromatograph. Ammonium was quantified colorimetrically (46). Aqueous Fe(II) was measured by adding an aliquot of supernatant directly to ferrozine (48) in the anaerobic chamber. Sorbed Fe(II) was measured by decanting the remaining supernatant and replacing it with an equal volume of 0.5 M HCl; the pellet was resuspended and placed on a shaker table at 100 rpm for 1 h, and Fe(II) in the extract was measured (after centrifugation) using ferrozine.

TEM. Fe(III) oxides from the batch reactors were recovered by centrifugation at 10,000 × g for 10 min and washed with anoxic deionized water. Samples were placed on copper grids, covered with a carbon-coated Formvar film, and examined with a Philips CM 200UT transmission electron microscope (spherical aberration coefficient, 0.5 mm; point-to-point resolution, 0.19 nm) equipped with Noran Voyager X-ray energy-dispersive spectroscopy (EDS).

RESULTS AND DISCUSSION

Nitrate-reducing cultures. Acetate and nitrate were consumed concomitantly in the acetate-limited, nitrate-reducing incubations (system 1) (Fig. 1A). Acetate was depleted by day 6, whereas some nitrate remained for the duration of the experiment. No increase in Fe(II) was observed, and the concentration remained similar to the background level of ca. 0.2 mM. These results indicate that denitrification was the dominant pathway for acetate metabolism in these cultures. This conclusion is consistent with the microbial community analysis data (Fig. 2B; see Fig. S1 in the supplemental material), which

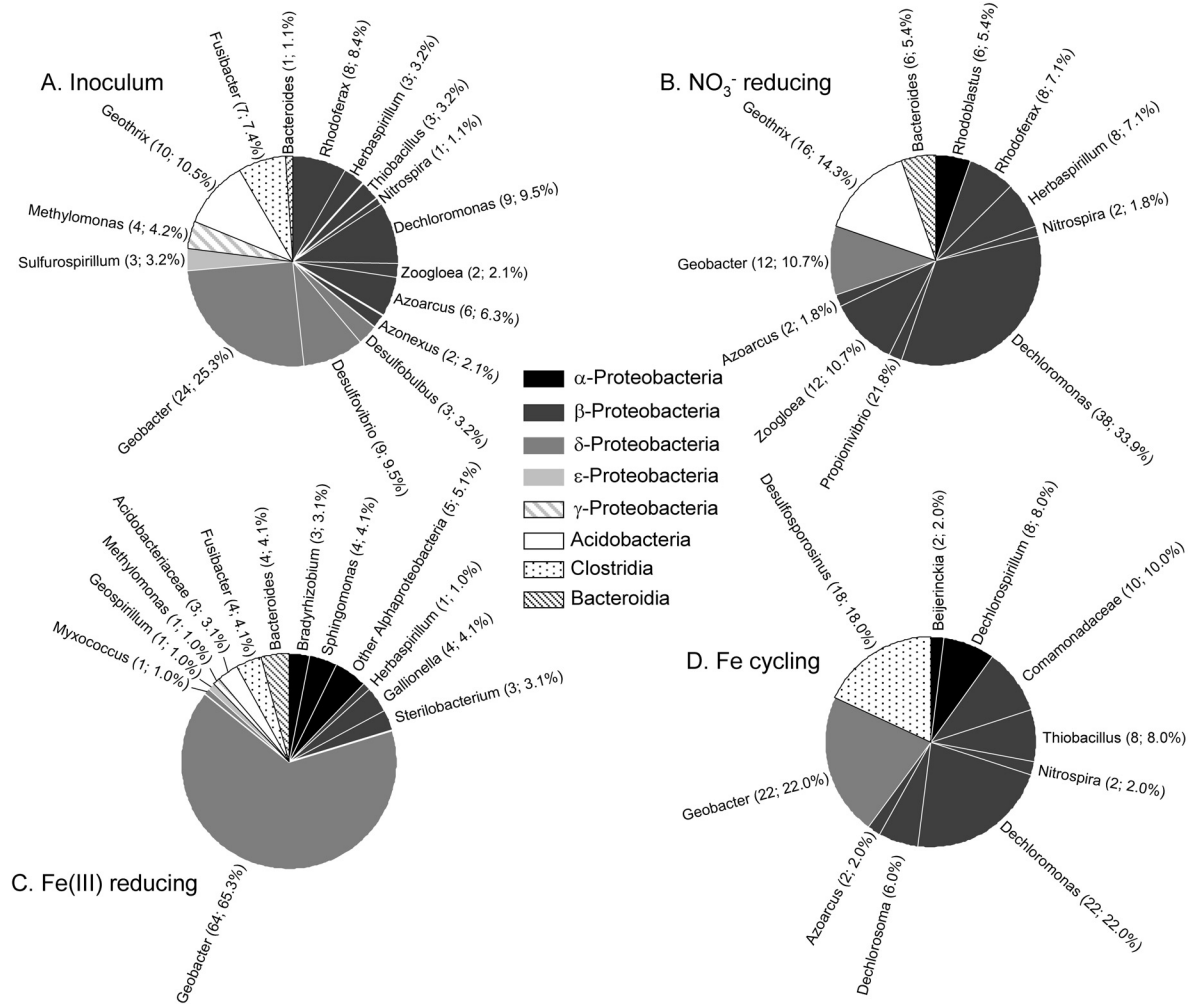


FIG. 2. Compositions of 16S rRNA gene clone libraries from the original sediment inoculum (95 clones) (A), the nitrate-reducing cultures after 11 days of incubation (112 clones) (B), the Fe(III)-reducing cultures after 18 days of incubation (98 clones) (C), and the Fe cycling cultures after 129 days of incubation (100 clones) (D). Numbers in parentheses indicate the number of clones for each taxonomic assignment and their percent abundance in the library.

showed a predominance of phylotypes related to known *Beta*-proteobacteria denitrifying taxa (e.g., *Dechloromonas*). After 18 days of incubation, the nitrate-reducing cultures contained substantial numbers of both acetate-oxidizing nitrate reducers and nitrate-dependent Fe(II) oxidizers that could grow with or without acetate (Table 1); lower but significant numbers of Fe(III)-reducing organisms were also detected. Four nitrate-reducing *Betaproteobacteria* were isolated from the acetate/nitrate cultures (see Table S1 in the supplemental material), each of which reduced nitrate without ammonium production when grown with 5 mM acetate and 5 mM nitrate. One of the cultures (UWNR4, a *Dechloromonas* strain) was able oxidize a significant amount (ca. 90%) of Fe(II) in mixotrophic medium containing 5 mM nitrate, 5 mM Fe(II), and 0.5 mM acetate (data not shown).

Fe(III)-reducing cultures. Approximately 6 mmol of HCl-extractable Fe(II) per liter was produced during metabolism of 1 mM acetate in the nitrate-free, Fe(III)-reducing (system 2) cultures (Fig. 1B). These cultures were dominated by *Geobac-*

TABLE 1. Roll tube enumeration results for the nitrate-reducing, Fe(III)-reducing, and Fe cycling cultures

Culture system	Electron donor, acceptor	Cell density (cells ml ⁻¹) ^a
1 (nitrate reducing)	Acetate, nitrate	3.4×10^7
	Acetate, Fe(III)	6.0×10^5
	Fe(II), nitrate	2.1×10^7
	Fe(II)/acetate, nitrate	1.5×10^8
2 [Fe(III) reducing]	Acetate, nitrate	ND ^b
	Acetate, Fe(III)	1.0×10^6
	Fe(II), nitrate	5.2×10^2
	Fe(II)/acetate, nitrate	4.0×10^2
3 (Fe cycling)	Acetate, nitrate	5.3×10^6
	Acetate, Fe(III)	1.5×10^7
	Fe(II), nitrate	7.2×10^6
	Fe(II)/acetate, nitrate	6.3×10^6

^a All cultures were incubated for 2 months prior to colony enumeration. Results are means for duplicate tubes; the ranges for duplicates were <5% of the means.

^b ND, not determined.

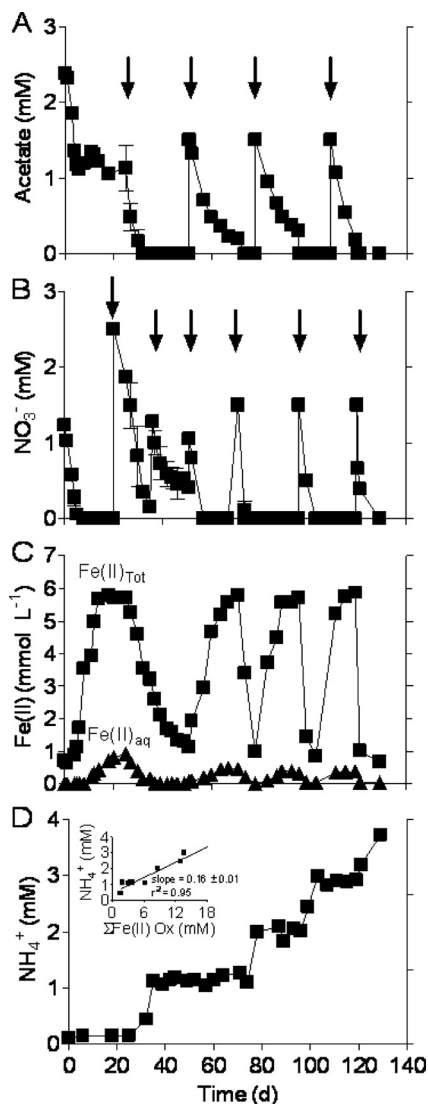


FIG. 3. Acetate (A) and nitrate (B) utilization, Fe(II) (total and aqueous) production and consumption (C), and ammonium accumulation (D) in the Fe cycling (system 3) cultures. The initial acetate and nitrate concentrations were 2.1 mM and 1.1 mM, respectively. Subsequent additions of acetate or nitrate (indicated by arrows) were dictated by the consumption of acetate or nitrate within the system. The inset in panel D shows the relationship between ammonium concentration and the cumulative amount of nitrate-dependent Fe(II) oxidation; the line shows the results of linear least-squares regression analysis. Data represent means for duplicate cultures.

ter phylotypes (Fig. 2C; see Fig. S1 in the supplemental material) and contained ca. 10^6 ml^{-1} of acetate-utilizing DIRB after 18 days of incubation (Table 1). The abundance of culturable nitrate-dependent Fe(II) oxidizers in the Fe(III)-reducing cultures was notably lower than that in the nitrate-reducing cultures (Table 1).

Fe redox cycling cultures. Fe(III) reduction commenced following nitrate depletion in the Fe cycling (system 3) cultures (Fig. 3), leading to the production of ca. 6 mmol per liter of Fe(II). Addition of nitrate at day 20 resulted in the rapid oxidation of Fe(II) and consumption of residual acetate. A

second nitrate addition at day 36 facilitated continued nitrate-dependent Fe(II) oxidation. Subsequent addition of acetate at day 50 led to rapid nitrate depletion followed by another pulse of Fe(III) reduction. Addition of nitrate at day 74 under acetate-depleted conditions led to rapid Fe(II) oxidation. Acetate added again 4 days later resulted in immediate regeneration of the Fe(II). Another nearly identical cycle of nitrate-driven Fe(II) oxidation and acetate-fueled Fe(III) reduction ensued, followed by a final round of Fe(II) oxidation. A total of four complete cycles of Fe reduction and oxidation were thus obtained in this experiment. The time needed to complete an Fe redox cycle decreased from about 50 days for the first cycle to 20 to 25 days in subsequent cycles, suggesting that Fe redox cycling populations were stimulated. Nitrate-dependent Fe(II) oxidation was associated with ammonium accumulation (Fig. 3D). Nitrite was detected only sporadically and always at concentrations less than $50 \mu\text{M}$, which suggests that nitrate was in general reduced directly to ammonium (or other reduced end products, e.g., N_2 ; see below).

The 4-month-old Fe cycling cultures yielded 15- to 20-fold more DIRB than the nitrate-reducing and Fe(III)-reducing cultures operated for a much shorter period (Table 1), which is consistent with the much larger total amount of Fe(III) oxide reduction activity that took place in the cycling reactors. The initial microbial community in the Fe cycling cultures closely resembled that in the nitrate-reducing cultures (see Fig. S1B and D in the supplemental material). DGGE revealed the development of a more diverse community during Fe redox cycling (see Fig. S1D to H in the supplemental material), which was confirmed by examination of the clone library constructed at the end of the experiment (Fig. 2D).

Mechanisms of anaerobic Fe redox cycling. Fe(II)-driven nitrate reduction produced ammonium, as observed in a previous analogous study (60). The overall molar ratio of ammonium produced to Fe(II) oxidized (0.17 ± 0.01) (Fig. 3D, inset) was similar to that expected for the oxidation of aqueous (Fe^{2+}) or surface-associated ($\equiv\text{O-Fe}^+$) Fe(II) coupled to reduction of nitrate to ammonium according to reactions such as $\text{Fe}^{2+} + 0.125\text{NO}_3^- + 1.625\text{H}_2\text{O} \rightarrow \text{FeOOH} + 0.125\text{NH}_4^+ + 1.75\text{H}^+$ and $\equiv\text{O-Fe}^+ + 0.125\text{NO}_3^- + 1.625\text{H}_2\text{O} \rightarrow \equiv\text{OH} + \text{FeOOH} + 0.125\text{NH}_4^+ + 0.75\text{H}^+$. This result suggested involvement of Fe(III)-reducing *Geobacter* species that are capable of oxidizing Fe(II) with reduction of nitrate to ammonium (60).

Extensive, but unsuccessful, attempts were made to recover pure cultures of *Geobacter* from acetate/goethite enrichments derived from the Fe redox cycling reactors in order to determine whether such organisms were capable of Fe(II) oxidation with reduction of nitrate to ammonium. Organisms from the *Rhodocyclaceae* (*Azospira* and *Dechloromonas*), the *Desulfovibrionaceae* (*Desulfovibrio*), and the *Sporomusa-Pectinatus-Selenomonas* phyletic group (*Anaerovibrio*) were recovered from colonies picked from roll tubes (see Table S1 in the supplemental material). None of these isolates grew via Fe(III) reduction [10 mM Fe(III)-NTA or 50 mmol liter⁻¹ of amorphous Fe(III) oxide] or oxidized significant amounts of Fe(II) in medium containing 5 mM nitrate, 5 mM Fe(II), and 0.5 mM acetate.

Despite the lack of recovered acetate-oxidizing DIRB, 16S rRNA gene clone libraries (ca. 800-bp fragments) showed that

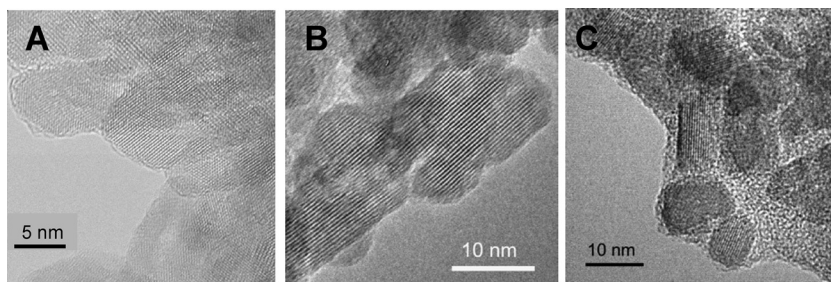


FIG. 4. High-resolution TEM images of samples collected at the ends of the nitrate-reducing (A), Fe(III)-reducing (B), and Fe redox cycling (C) experiments. Note the marked increase in the abundance of amorphous material surrounding and among goethite nanocrystals in the sample from the Fe redox cycling reactor (C).

the three goethite-reducing enrichment cultures (25 clones each) were dominated by an operational taxonomic unit (OTU) 95% similar to *Geobacter pelophilus* (50). These sequences were 99% similar to several *Geobacter*-related OTUs recovered in 16S rRNA gene libraries from the Fe redox cycling cultures. The three acetate/goethite enrichment cultures were tested for the ability to oxidize Fe(II) with nitrate following an initial period of acetate-limited Fe(III) reduction. These experiments were carried out with cells grown on Fe-rich smectite, which proved to be the best substrate for growth of the later, less robust generations of the enrichments. Cells for these experiments were obtained by transferring the goethite-reducing enrichments to a suspension of specimen smectite (NaU-2) in standard culture medium and growing them for three generations prior to addition of nitrate to acetate-depleted cultures. All three cultures showed significant Fe(II) oxidation activity [20 to 35% of the available Fe(II)] in the presence of excess nitrate. These results support the inference that *Geobacter*-related DIRB participated in nitrate-dependent Fe(II) oxidation in the Fe redox cycling cultures.

Organisms from the *Betaproteobacteria* known to be capable of nitrate-dependent Fe(II) oxidation (e.g., *Dechloromonas*, *Dechlorosoma*, and *Thiobacillus* [59]) were also detected in the Fe redox cycling reactors (Fig. 2D; see Fig. S1 in the supplemental material). The quantitative role of these taxa in Fe(II) oxidation is uncertain, given that all known betaproteobacterial nitrate-dependent Fe(II) oxidizers produce N₂ rather than ammonium as the end product of nitrate reduction (59). It is important to note, however, that the ratio of nitrate consumed to Fe(II) oxidized during the last three periods of Fe(II) oxidation (0.25 ± 0.02 ; see Fig. S2A in the supplemental material), when no acetate was present, was twice that expected for Fe(II) oxidation coupled to reduction of nitrate to ammonium. This result suggests that some of the nitrate consumed during these periods was linked to organotrophic metabolism, e.g., endogenous respiration and/or oxidation of dead bacterial biomass. This conclusion raises the possibility that some of the ammonium accumulation during nitrate-dependent Fe(II) oxidation was linked to organotrophy (e.g., by nitrate-reducing *Geobacter*) rather than Fe(II) oxidation, which in turn suggests that some of the nitrate-driven Fe(II) oxidation activity could have been carried out by betaproteobacterial denitrifiers as opposed to *Geobacter*, including both heterotrophic (e.g., *Dechloromonas* and *Dechlorosoma*) and autotrophic (e.g., *Thiobacillus*) taxa.

The Solver tool in Microsoft Excel was used to constrain the possible quantitative significance of these different pathways for nitrate reduction. The ratio of nitrate consumed to Fe(II) oxidized during the last three periods of Fe(II) oxidation was fixed at the observed value of 0.253 (see Fig. S2A in the supplemental material). The presumed rate of organotrophic nitrate reduction, along with the fraction of nitrate reduced to N₂ versus ammonium during organotrophic and lithotrophic [Fe(II)-driven] nitrate reduction, was then varied within the Solver routine to reproduce the observed ratio of ammonium produced to Fe(II) oxidized during the last three periods of Fe(II) oxidation (0.182; see Fig. S2B in the supplemental material). A summary of the calculation procedure and results is provided in Table S2 in the supplemental material. The results indicated a rate of organotrophic nitrate reduction equivalent to 46% of total nitrate consumption, with 68% of organotrophic nitrate reduction and 83% of Fe(II)-driven nitrate reduction resulting in ammonium production. The percentage of Fe(II) oxidation coupled to reduction of nitrate to ammonium was 76% of the total amount. These calculations lend conceptual support to the hypothesis suggested by the DGGE and clone library results, i.e., that nitrate-driven Fe(II) oxidation was carried out by both betaproteobacterial denitrifiers and ammonium-producing *Geobacter* spp. in the Fe cycling reactors.

Influence of Fe redox cycling on Fe(III) oxide mineralogy. High-resolution TEM analysis demonstrated the presence of goethite nanocrystals less than 30 nm in length and 10 nm in diameter (Fig. 4). Selected area electron diffraction patterns indicated the relatively low crystallinity of the goethite and the absence of major mineral-phase transformations during reduction or Fe redox cycling (see Fig. S3 in the supplemental material). These results are consistent with a prior study (60) which showed that nitrate-dependent oxidation of microbially reduced goethite did not result in the formation of new crystalline Fe(III) oxide phases. However, TEM images of samples from the Fe redox cycling cultures did show ubiquitous amorphous material surrounding the goethite nanocrystals that were absent in the nitrate- and Fe(III)-reducing systems (Fig. 4). To our knowledge this is the first demonstration of the generation of amorphous Fe(III) oxide coatings on otherwise crystalline Fe(III) oxide mineral phases during nitrate-dependent Fe(II) oxidation. These results are consistent with the view that Fe redox cycling is likely to result in the formation of highly reactive, amorphous Fe(III) oxide phases (55), and they

may explain the observed production of small quantities of dilute HCl-extractable (presumably amorphous) Fe(III) oxide during nitrate-dependent oxidation of microbially reduced goethite by sediment microflora and *Geobacter metallireducens* (60).

Environmental implications. Our experiments show that a microbial system undergoing repeated temporal oscillations in the input of organic carbon and nitrate developed a community structure capable of mediating sustained anaerobic Fe redox cycling through dissimilatory Fe(III) oxide reduction and nitrate-dependent Fe(II) oxidation. These results are analogous to those of a previous experiment with natural-sediment microflora in which Fe went through a single cycle of Fe reduction and oxidation (60) and to those of experiments with cocultures of *Geobacter bremsensis* (53) or *Geobacter sulfurreducens* (7) (neither of which reduce nitrate) and the lithoautotrophic nitrate-reducing, Fe(II)-oxidizing enrichment culture of Straub et al. (52). Together these studies suggest that microbial Fe cycling communities are likely to be present and active in anoxic soil and sedimentary environments experiencing shifts in organic carbon and nitrate input, analogous to those known to be present in aerobic/anaerobic interfacial environments (6, 8, 23, 47). When inputs of organic carbon are high compared to nitrate, organic carbon oxidation by nitrate-reducing bacteria exhausts available nitrate, thus allowing microbial Fe(III) reduction to become the predominant TEAP (4, 32, 34, 57). During subsequent periods of reduced organic carbon loading, rates of nitrate resupply may exceed rates of organotrophic nitrate reduction, resulting in the potential for lithotrophic, nitrate-dependent Fe(II) oxidation, e.g., at the redox boundary in nitrate-contaminated aquifers in agricultural areas (17, 18, 39) or at the fringe of the Fe(III) reduction zone in organic-contaminated aquifers (2, 14, 56). A similar coupling of N and Fe redox may take place in freshwater or marine surface sediments (27, 51). In each of these situations, reducing equivalents stored in the form of Fe(II)-bearing solid phases (including, in some cases, iron sulfide minerals [9, 22]) may eventually serve as a significant source of energy for lithotrophic microbial metabolism during periods of reduced organic carbon input or during bioturbation- or wave-induced mixing of aquatic surface sediments. The importance of solid-associated Fe(II) in Fe redox cycling is illustrated by the fact that aqueous Fe(II) accounted for less than 20% of total Fe(II) production and oxidation in the Fe(III)-reducing and Fe cycling cultures (Fig. 1B and 3C).

A key aspect of this study and the previous related study (60) is that ammonium was a major end product of nitrate-dependent Fe(II) oxidation during anaerobic Fe redox cycling. This finding has important implications for the fate of N in sediments, as ammonium so produced may eventually be returned to surface waters where it could serve as nutrient for algal and higher plant production. In contrast, conversion of nitrate to N₂ effectively represents a loss of N from the sedimentary N cycle (45). Recent studies suggest that this dissimilatory reduction of nitrate to ammonium may also occur during sulfide-linked nitrate reduction in freshwater wetland sediments (9, 38). Finally, given the fundamental influence of Fe(III) oxide surface area and crystallinity on rates of microbial Fe(III) reduction (41), changes in Fe(III) oxide mineralogy (e.g., production of amorphous surface coatings) associated with micro-

bial Fe redox cycling have the potential to alter the reactivity of Fe(III) oxides in soils and sediments.

ACKNOWLEDGMENTS

We thank Marco Blöthe for his help with 16S rRNA gene sequence analyses and Jason Flagg (Indiana University) for assistance with microbial isolations.

This research was supported by grant 0525510 from the NSF Biogeosciences Program and grants DE-FG02-06ER64184 and ER64172-1027487-001191 from the Office of Biological and Environmental Research, U.S. Department of Energy, Office of Science.

REFERENCES

- Altschul, S. F., et al. 1997. Gapped BLAST and PSI-BLAST: a new generation of protein database search programs. *Nucleic Acids Res.* **25**:3389–3402.
- Amirbahman, A., R. Schonenberger, C. A. Johnson, and L. Sigg. 1998. Aqueous- and solid-phase biogeochemistry of a calcareous aquifer system downgradient from a municipal solid waste landfill (Winterthur, Switzerland). *Environ. Sci. Technol.* **32**:1933–1940.
- Baedecker, M. J., and W. Back. 1979. Modern marine sediments as a natural analog to the chemically stressed environment of a landfill. *J. Hydrol.* **43**:393–414.
- Baker, M. A., C. N. Dahm, and H. M. Valett. 1999. Acetate retention and metabolism in the hyporheic zone of a mountain stream. *Limnol. Oceanogr.* **44**:1530–1539.
- Benz, M., A. Brune, and B. Schink. 1998. Anaerobic and aerobic oxidation of ferrous iron at neutral pH by chemoheterotrophic nitrate-reducing bacteria. *Arch. Microbiol.* **169**:159–165.
- Blöthe, M., and E. E. Roden. 2009. Microbial iron redox cycling in a circum-neutral-pH groundwater seep. *Appl. Environ. Microbiol.* **75**:468–473.
- Blöthe, M., and E. E. Roden. 2009. Composition and activity of an autotrophic Fe(II)-oxidizing, nitrate-reducing enrichment culture. *Appl. Environ. Microbiol.* **75**:6937–6940.
- Braun, A. M., K. Finster, H. P. Gunlaugsson, P. Nrnberg, and M. W. Friedrich. 2010. A comprehensive investigation on iron cycling in a freshwater seep including microscopy, cultivation and molecular community analysis. *Geomicrobiol. J.* **27**:15–34.
- Burgin, A. J., and S. K. Hamilton. 2008. NO₃⁻-driven SO₄²⁻ production in freshwater ecosystems: implications for N and S cycling. *Ecosystems* **11**:908–922.
- Chang, Y. J., et al. 2000. Phylogenetic analysis of aerobic freshwater and marine enrichment cultures efficient in hydrocarbon degradation: effect of profiling method. *J. Microbiol. Methods* **40**:19–31.
- Chapelle, F. H. 2000. The significance of microbial processes in hydrogeology. *Hydrogeol. J.* **8**:41–46.
- Chapelle, F. H. 2001. *Ground-water microbiology and geochemistry*, 2nd ed. John Wiley & Sons, Inc., New York, NY.
- Chaudhuri, S. K., J. G. Lack, and J. D. Coates. 2001. Biogenic magnetite formation through anaerobic biooxidation of Fe(II). *Appl. Environ. Microbiol.* **67**:2844–2848.
- Christensen, T. H., et al. 2000. Characterization of redox conditions in groundwater contaminant plumes. *J. Contam. Hydrol.* **45**:165–241.
- Cornell, R. M., and U. Schwertmann. 1996. *The iron oxides*. VCH Verlagsgesellschaft mbH/VCH Publishers, Inc., Weinheim, Germany.
- Davison, W., and G. Seed. 1983. The kinetics of the oxidation of ferrous iron in synthetic and natural waters. *Geochim. Cosmochim. Acta* **47**:67–79.
- Ernstsen, V., S. Binnerup, and J. Sorensen. 1998. Reduction of nitrate in clayey subsoils controlled by geochemical and microbial barriers. *Geomicrobiol. J.* **15**:195–207.
- Ernstsen, V., W. P. Gates, and J. W. Stucki. 1998. Microbial reduction of structural iron in clays—a renewable source of reduction capacity. *J. Environ. Qual.* **27**:761–766.
- Forshay, K. J., and E. H. Stanley. 2005. Rapid nitrate loss and denitrification in a temperate river floodplain. *Biogeochemistry* **75**:43–64.
- Froelich, P. N., et al. 1979. Early oxidation of organic matter in pelagic sediments of the eastern equatorial Atlantic: suboxic diagenesis. *Geochim. Cosmochim. Acta* **43**:1075–1090.
- Gillis, M., P. Vandamme, P. DeVos, J. Swings, and K. Kersters. 2001. Polyphasic taxonomy, p. 43–48. *In* D. R. Boone and R. W. Castenholz (ed.), *Bergey's manual of systematic bacteriology*, 2nd ed., vol. 1. Springer, New York, NY.
- Haaijer, S. C. M., L. P. M. Lamers, A. J. P. Smolders, M. S. M. Jetten, and H. J. M. O. denCamp. 2007. Iron sulfide and pyrite as potential electron donors for microbial nitrate reduction in freshwater wetlands. *Geomicrobiol. J.* **24**:391–401.
- Haaijer, S. C. M., et al. 2008. Bacteria associated with iron seeps in a sulfur-rich, neutral pH, freshwater ecosystem. *ISME J.* **2**:1231–1242.
- Hall, T. 1999. BioEdit: a user-friendly biological sequence alignment editor and analysis program for Windows 95/98/NT. *Nucleic Acids Symp. Ser.* **41**:95–98.

25. Hauck, S., M. Benz, A. Brune, and B. Schink. 2001. Ferrous iron oxidation by denitrifying bacteria in profundal sediments of a deep lake (Lake Constance). *FEMS Microb. Ecol.* **37**:127–134.
26. Hungate, R. E. 1969. A roll tube method for cultivation of strict anaerobes. *Methods Microbiol.* **3B**:117–132.
27. Jorgensen, B. B. 2000. Bacteria and marine biogeochemistry, p. 173–207. In H. D. Schulz and M. Zabel (ed.), *Marine geochemistry*. Springer, New York, NY.
28. Klüber, H. D., and R. Conrad. 1998. Effects of nitrate, nitrite, NO, and N₂O on methanogenesis and other redox processes in anoxic rice soil. *FEMS Microbiol. Ecol.* **25**:301–318.
29. Lovley, D. R., and E. J. P. Phillips. 1986. Organic matter mineralization with reduction of ferric iron in anaerobic sediments. *Appl. Environ. Microbiol.* **51**:683–689.
30. Lovley, D. R., and E. J. P. Phillips. 1987. Rapid assay for microbially reducible ferric iron in aquatic sediments. *Appl. Environ. Microbiol.* **53**:1536–1540.
31. Lovley, D. R., and E. J. P. Phillips. 1988. Manganese inhibition of microbial iron reduction in anaerobic sediments. *Geomicrobiol. J.* **6**:145–155.
32. Massmann, G., A. Pekdeger, and C. Merz. 2004. Redox processes in the Oderbruch polder groundwater flow system in Germany. *Appl. Geochem.* **19**:863–886.
33. Millero, F. J., S. Sotolongo, and M. Izaguirre. 1987. The oxidation kinetics of Fe(II) in seawater. *Geochim. Cosmochim. Acta* **51**:793–801.
34. Morrice, J. A., C. N. Dahm, H. M. Valett, P. V. Unnikrishna, and M. E. Campana. 2000. Terminal electron-accepting processes in the alluvial sediments of a headwater stream. *J. N. Am. Benthol. Soc.* **19**:593–608.
35. Muyzer, G., A. Teske, C. O. Wirsen, and H. W. Jannasch. 1995. Phylogenetic relationships of *Thiomicrospira* species and their identification in deep-sea hydrothermal vent samples by denaturing gradient gel electrophoresis of 16S rDNA fragments. *Arch. Microbiol.* **164**:165–172.
36. Myers, C. R., and K. H. Neelson. 1988. Microbial reduction of manganese oxides: interactions with iron and sulfur. *Geochim. Cosmochim. Acta* **52**:2727–2732.
37. Nielsen, J. L., and P. H. Nielsen. 1998. Microbial nitrate-dependent oxidation of ferrous iron in activated sludge. *Environ. Sci. Technol.* **32**:3556–3561.
38. Payne, E. K., A. J. Burgin, and S. K. Hamilton. 2009. Sediment nitrate manipulation using porewater equilibrators reveals potential for N and S coupling in freshwaters. *Aquat. Microb. Ecol.* **54**:233–241.
39. Postma, D., C. Boesen, H. Kristiansen, and F. Larsen. 1991. Nitrate reduction in an unconfined sandy aquifer: water chemistry, reduction processes, and geochemical modeling. *Wat. Resour. Res.* **27**:2027–2045.
40. Ratering, S., and S. Schnell. 2001. Nitrate-dependent iron(II) oxidation in paddy soil. *Environ. Microbiol.* **3**:100–109.
41. Roden, E. E. 2003. Fe(III) oxide reactivity toward biological versus chemical reduction. *Environ. Sci. Technol.* **37**:1319–1324.
42. Roden, E. E. 2006. Geochemical and microbiological controls on dissimilatory iron reduction. *C. R. Geosci.* **338**:456–467.
43. Roden, E. E., and J. M. Zachara. 1996. Microbial reduction of crystalline iron(III) oxides: influence of oxide surface area and potential for cell growth. *Environ. Sci. Technol.* **30**:1618–1628.
44. Schwertmann, U., and R. M. Cornell. 1991. *Iron oxides in the laboratory*. VCH Verlagsgesellschaft mbH/VCH Publishers, Inc., Weinheim, Germany.
45. Seitzinger, S. P. 1988. Denitrification on freshwater and coastal marine ecosystems: ecological and geochemical significance. *Limnol. Oceanogr.* **33**:702–724.
46. Sims, G., T. Ellsworth, and R. Mulyaney. 1995. Microscale determination of inorganic nitrogen in water and soil extracts. *Commun. Soil Sci. Plant Anal.* **26**:303–316.
47. Sobolev, D., and E. E. Roden. 2002. Evidence for rapid microscale bacterial redox cycling of iron in circumneutral environments. *Antonie Van Leeuwenhoek* **181**:587–597.
48. Stookey, L. L. 1970. Ferrozine—a new spectrophotometric reagent for iron. *Anal. Chem.* **42**:779–781.
49. Straub, K. L., and B. E. E. Buchholz-Cleven. 1998. Enumeration and detection of anaerobic ferrous-iron oxidizing, nitrate-reducing bacteria from diverse European sediments. *Appl. Environ. Microbiol.* **64**:4846–4856.
50. Straub, K. L., and B. E. E. Buchholz-Cleven. 2001. *Geobacter brementis* sp. nov. and *Geobacter pelophilus* sp. nov., two dissimilatory ferric-iron-reducing bacteria. *Int. J. Syst. Evol. Microbiol.* **51**:1805–1808.
51. Straub, K. L., M. Benz, and B. Schink. 2001. Iron metabolism in anoxic environments at near neutral pH. *FEMS Microbiol. Ecol.* **34**:181–186.
52. Straub, K. L., M. Benz, B. Schink, and F. Widdel. 1996. Anaerobic, nitrate-dependent microbial oxidation of ferrous iron. *Appl. Environ. Microbiol.* **62**:1458–1460.
53. Straub, K. L., W. A. Schonhuber, B. E. E. Buchholz-Cleven, and B. Schink. 2004. Diversity of ferrous iron-oxidizing, nitrate-reducing bacteria and their involvement in oxygen-independent iron cycling. *Geomicrobiol. J.* **21**:371–378.
54. Thompson, A., O. A. Chadwick, D. G. Rancourt, and J. Chorover. 2006. Iron-oxide crystallinity increases during soil redox oscillations. *Geochim. Cosmochim. Acta* **70**:1710–1727.
55. van Breemen, N. 1988. Long-term chemical, mineralogical and morphological effects of iron-redox processes in periodically flooded soils, p. 811–823. In J. W. Stucki, B. A. Goodman, and U. Schwertmann (ed.), *Iron in soils and clay minerals*. D. Reidel Publishing Co., Boston, MA.
56. van Breukelen, B. M., and J. Griffioen. 2004. Biogeochemical processes at the fringe of a landfill leachate pollution plume: potential for dissolved organic carbon, Fe(II), Mn(II), NH₄, and CH₄ oxidation. *J. Contam. Hydrol.* **73**:181–205.
57. von Gunten, H. R., G. Karametaxas, and R. Keil. 1994. Chemical processes in infiltrated riverbed sediments. *Environ. Sci. Technol.* **28**:2087–2093.
58. Weber, K. A., F. W. Picardal, and E. E. Roden. 2001. Microbially-catalyzed nitrate-dependent oxidation of biogenic solid-phase Fe(II) compounds. *Environ. Sci. Technol.* **35**:1644–1650.
59. Weber, K. A., L. A. Achenbach, and J. D. Coates. 2006. Microorganisms pumping iron: anaerobic microbial iron oxidation and reduction. *Nat. Rev. Microbiol.* **4**:752–764.
60. Weber, K. A., P. F. Churchill, M. M. Urrutia, R. K. Kukkadapu, and E. E. Roden. 2006. Anaerobic redox cycling of iron by wetland sediment microorganisms. *Environ. Microbiol.* **8**:100–113.
61. Zachara, J. M., R. K. Kukkadapu, J. K. Fredrickson, Y. A. Gorby, and S. C. Smith. 2002. Biomineralization of poorly crystalline Fe(III) oxides by dissimilatory metal reducing bacteria (DMRB). *Geomicrobiol. J.* **19**:179–207.

Supplemental material

Repeated Anaerobic Microbial Redox Cycling of Iron

Aaron J. Coby^{1, ‡}, Flynn Picardal², Evgenya Shelobolina¹, Huifang Xu¹, and Eric E. Roden^{1*}

¹ *Department of Geoscience, University of Wisconsin, Madison, WI 53706;*

² *School of Public and Environmental Affairs, Indiana University, Bloomington, IN 47405*

Table S1. Origin and characteristics of pure culture isolates.

Isolate(s)	Source	Isolation medium	Phylogenetic assignment	Matches to clone library sequences	NO ₃ ⁻ Red? ^a	Fe(III) Red? ^b	Fe(II) Ox? ^c
			Class, Family, Genus species Accession no.; % Similarity; No. bp				
UWNR1	System 1 acetate/NO ₃ ⁻ enrichment culture	Acetate/NO ₃ ⁻ plates	<i>Betaproteobacteria, Oxalobacteraceae</i> <i>Janthinobacterium</i> sp. Everest-gws-74 EU584527; 92%; 1239	91% similar to 2 clones from system 3	Y	N	N
UWNR2	System 1 acetate/NO ₃ ⁻ enrichment culture	Acetate/NO ₃ ⁻ plates	<i>Betaproteobacteria, Rhodocyclaceae</i> <i>Dechloromonas hortensis</i> strain MA-1 AY277621; 95%; 1233	97-99% similar to 7 clones from system 3	Y	N	N
UWNR3	System 1 acetate/NO ₃ ⁻ enrichment culture	Acetate/NO ₃ ⁻ plates	<i>Betaproteobacteria, Rhodocyclaceae</i> <i>Dechloromonas hortensis</i> strain MA-1 AY277621; 96%; 1256	99-100% similar to 17 clones from original material, system 1, and system 3	Y	N	N
UWNR4	System 1 acetate/NO ₃ ⁻ enrichment culture	Acetate/NO ₃ ⁻ plates	<i>Betaproteobacteria, Rhodocyclaceae</i> <i>Dechloromonas hortensis</i> strain MA-1 AY277621; 96%; 1256	98-100% similar to 17 clones from original material, system 1, and system 3	Y	N	N
Fs1a, Fs1f, Fs1g	System 1 acetate/goethite enrichment culture	Acetate/HFO roll tubes	<i>Betaproteobacteria, Rhodocyclaceae</i> <i>Azospira oryzae</i> strain N1 DQ863512, 99%; 1367	94-95% similar to 3 clones from original material and system 1	Y	N	N
Fg10, Fg15, Fg18, Fg19, Fg20	System 2 acetate/goethite enrichment culture	Acetate/HFO roll tubes	<i>Betaproteobacteria, Rhodocyclaceae</i> <i>Dechloromonas agitata</i> strain CKB AF047462 (97%), 1395	95-99% similar to 12 clones from original material, system 1 and 3	Y	N	N
Fg2, Fg7, Fg8	System 2 acetate/goethite enrichment culture	Acetate/HFO roll tubes	<i>Sporomusa-Pectinatus-Selenomonas</i> phyletic group, <i>Anaerovibrio burkinabensis</i> DSM 6283(T) AJ010961 (92%), 1319	Less than 90% similar to clones from system 2	N	Y ^d	N
FNTA4, FNTA6, FNTA7, FNTA8, FNTA4	System 2 acetate/Fe(III)-NTA enrichment culture	Acetate/nfa mix roll tubes	<i>Betaproteobacteria, Rhodocyclaceae</i> <i>Dechloromonas agitata</i> strain CKB AF047462 (97%), 1377	95-99% similar to 12 clones from original material, system 1 and 3	Y	N	N

FNTA3	System 2 acetate/Fe(III)-NTA enrichment culture	Acetate/nfa mix roll tubes	<i>Sporomusa-Pectinatus-Selenomonas</i> phyletic group, <i>Anaerovibrio burkinabensis</i> DSM 6283(T) AJ010961 (91%), 1307	Less than 90% similar to clones from system 2	N	Y ^d	N
Fs3c, Fs3h	System 3 acetate/goethite enrichment culture	Acetate/HFO roll tubes	<i>Betaproteobacteria, Rhodocyclaceae</i> <i>Azospira oryzae</i> strain N1 DQ863512 , 99%; 1345	94-95% similar to 3 clones from original material (om24) and system 1 (I-15 and I-17)	Y	N	N
Fs3_2	System 3 acetate/goethite enrichment culture	Acetate/HFO roll tubes	<i>Deltaproteobacteria, Desulfovibrionaceae,</i> <i>Desulfovibrio magneticus</i> strain DSM 13731 DVURS1 (98%), 1201	Less than 90% similar to clones from system 2	N	N	N

^a Colonies transferred to liquid medium with 5 mM nitrate/10 mM acetate.

^b Colonies transferred to liquid medium with 10 mM acetate/10 mM Fe(III)-NTA, or nfa mix (see Materials and Methods); no colonies grew in acetate/Fe(III)-NTA medium. Colonies that grew in nfa mix were tested for purity (microscopic analysis and 16S rRNA gene screening), and mixed cultures were discarded; pure cultures were transferred to liquid medium with 10 mM acetate/10 mM Fe(III)-NTA.

^c Colonies transferred from nfa mix to 10 mM nitrate/10 mM acetate; after growth transfer (10% vol/vol) to medium with 5 mM nitrate/5 mM Fe(II), with ca. 1 mM acetate introduced with transfer.

^d In the presence of 0.05 g L⁻¹ yeast extract only.

Table S2. Summary of calculations to constrain relative rates and pathways (denitrification vs. ammonium production) of organotrophic vs. lithotrophic (Fe(II)-driven) nitrate reduction in the Fe cycling cultures.

1. Arbitrarily set rate of nitrate-dependent Fe(II) oxidation ($R_{\text{Fe(II)}}$) at $1 \text{ mmol L}^{-1} \text{ d}^{-1}$; any value could be used since all rates are normalized to this rate.
2. Assume that the experimentally-observed ratio of nitrate consumed to Fe(II) oxidized ($R_{\text{NO}_3, \text{Tot}}/R_{\text{Fe(II)}} = 0.253$; Fig. S1A) represents the sum of organotrophic and lithotrophic (Fe(II)-driven) nitrate reduction.
3. Let $R_{\text{NO}_3, \text{organo}}$ represent the total rate of organotrophic nitrate reduction, which will be apportioned between reduction to N_2 vs. ammonium; **$R_{\text{NO}_3, \text{organo}}$ is varied during the solution procedure.**
4. Let $f_{\text{N}_2, \text{organo}}$ represent the fraction of nitrate reduced to N_2 during organotrophic reduction, and $f_{\text{N}_2, \text{litho}}$ represent the fraction of nitrate reduced to N_2 during lithotrophic reduction; **$f_{\text{N}_2, \text{organo}}$ and $f_{\text{N}_2, \text{litho}}$ are varied during the solution procedure.**
5. From 4 it follows that the fraction of nitrate reduced to ammonium during lithotrophic or organotrophic reduction is as follows: $f_{\text{NH}_4, \text{organo}} = (1 - f_{\text{N}_2, \text{organo}})$; $f_{\text{NH}_4, \text{litho}} = (1 - f_{\text{N}_2, \text{litho}})$; **$f_{\text{NH}_4, \text{organo}}$ and $f_{\text{NH}_4, \text{litho}}$ are directly tied to variations in $f_{\text{N}_2, \text{organo}}$ and $f_{\text{N}_2, \text{litho}}$ during the solution procedure.**
6. Calculate rates of organotrophic and lithotrophic nitrate reduction to N_2 or ammonium as follows:

$$\begin{aligned} R_{\text{NO}_3 \rightarrow \text{N}_2, \text{organo}} &= R_{\text{NO}_3, \text{organo}} \times f_{\text{N}_2, \text{organo}} \\ R_{\text{NO}_3 \rightarrow \text{NH}_4, \text{organo}} &= R_{\text{NO}_3, \text{organo}} \times f_{\text{NH}_4, \text{organo}} \\ R_{\text{NO}_3 \rightarrow \text{N}_2, \text{litho}} &= R_{\text{Fe(II)}} \times f_{\text{N}_2, \text{litho}} \times 0.2 \\ R_{\text{NO}_3 \rightarrow \text{NH}_4, \text{litho}} &= R_{\text{Fe(II)}} \times f_{\text{NH}_4, \text{litho}} \times 0.125 \end{aligned}$$

where 0.2 and 0.125 are the moles of nitrate required to oxidize one mole of Fe(II) with reduction to N_2 or ammonium, respectively.

7. Using the Solver routine in Microsoft Excel, search for values of $R_{\text{NO}_3, \text{organo}}$, $f_{\text{N}_2, \text{organo}}$, and $f_{\text{N}_2, \text{litho}}$ (together with $f_{\text{NH}_4, \text{organo}}$, and $f_{\text{NH}_4, \text{litho}}$; see step 5) that make the ratio of total ammonium production to Fe(II) oxidation $[(R_{\text{NO}_3 \rightarrow \text{NH}_4, \text{organo}} + R_{\text{NO}_3 \rightarrow \text{NH}_4, \text{litho}})/R_{\text{Fe(II)}}]$ equal to the experimentally-observed ratio of 0.182 (Fig. S1B), under the constraint that the ratio of total nitrate consumption to Fe(II) oxidation $[(R_{\text{NO}_3 \rightarrow \text{N}_2, \text{organo}} + R_{\text{NO}_3 \rightarrow \text{NH}_4, \text{organo}} + R_{\text{NO}_3 \rightarrow \text{N}_2, \text{litho}} + R_{\text{NO}_3 \rightarrow \text{NH}_4, \text{litho}})/R_{\text{Fe(II)}}]$ is equal to the experimentally-observed ratio of 0.253 (Fig. S1A).

Print-out of Excel spreadsheet showing calculation results (see next page):

Table S2, continued

Fixed values	
$R_{\text{Fe(II)}} =$	1.000

Varied values	
$R_{\text{NO}_3, \text{organo}} =$	0.115
$f_{\text{N}_2, \text{organo}} =$	0.325
$f_{\text{N}_2, \text{litho}} =$	0.167
$f_{\text{NH}_4, \text{organo}} =$	0.675
$f_{\text{NH}_4, \text{litho}} =$	0.833

Calculated rates	
$R_{\text{NO}_3 \rightarrow \text{N}_2, \text{organo}} =$	0.0375
$R_{\text{NO}_3 \rightarrow \text{NH}_4, \text{organo}} =$	0.0779
$R_{\text{NO}_3 \rightarrow \text{N}_2, \text{litho}} =$	0.0335
$R_{\text{NO}_3 \rightarrow \text{NH}_4, \text{litho}} =$	0.1041

Target values	
$R_{\text{NO}_3, \text{Tot}}/R_{\text{Fe(II)}} =$	0.253
$R_{\text{NH}_4}/R_{\text{Fe(II)}} =$	0.182

Derived rates and ratios	
$R_{\text{NO}_3, \text{organo, Tot}}/R_{\text{NO}_3, \text{Tot}} =$	0.456
$R_{\text{NO}_3, \text{litho, Tot}}/R_{\text{NO}_3, \text{Tot}} =$	0.544
$R_{\text{NO}_3 \rightarrow \text{NH}_4, \text{litho}}/R_{\text{NO}_3, \text{litho, Tot}} =$	0.757

Fig. S1

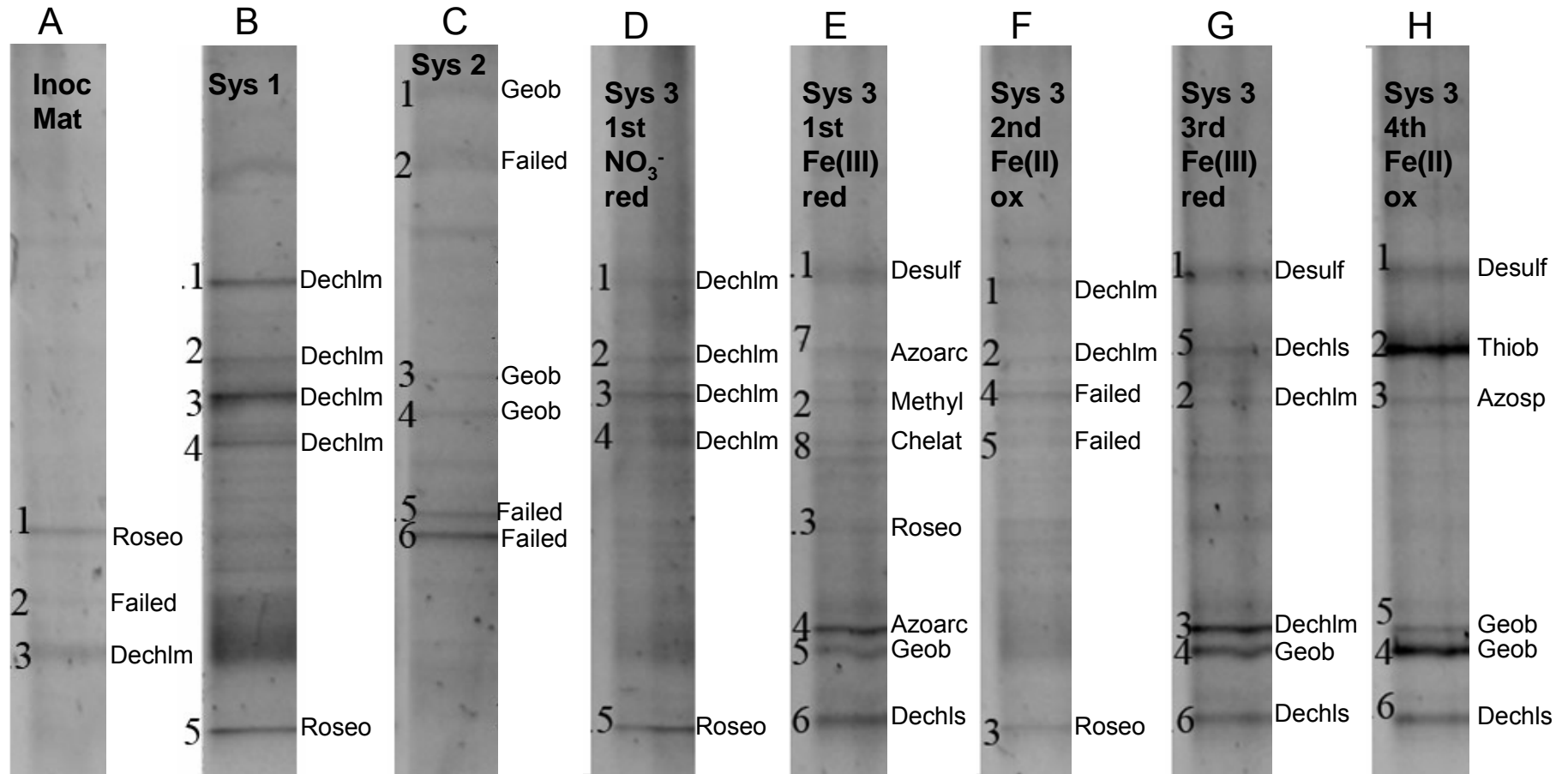


FIG. S1. DGGE analysis of 16S rRNA gene amplicons retrieved from the original sediment inoculum (A), the nitrate-reducing cultures (Sys 1) after 11 days of incubation (B), the Fe(III)-reducing cultures (Sys 2) after 18 days of incubation (C), and the Fe cycling cultures (Sys 3) after 10 (D), 21 (E), 78 (F), 96 (G), or 130 (H) days of incubation (100 clones). The names to the right of bands are abbreviations of taxa assigned by BLAST analysis of sequenced bands; “Failed” refers to bands for which sequencing was not successful. Abbreviations: Roseo = *Roseobacter*; Dechlm = *Dechloromonas*; Geob = *Geobacter*; Desulf = *Desulfovibrio*; Azoarc = *Azoarcus*; Dechls = *Dechlorosoma*; Thiob = *Thiobacillus*.

Fig. S2

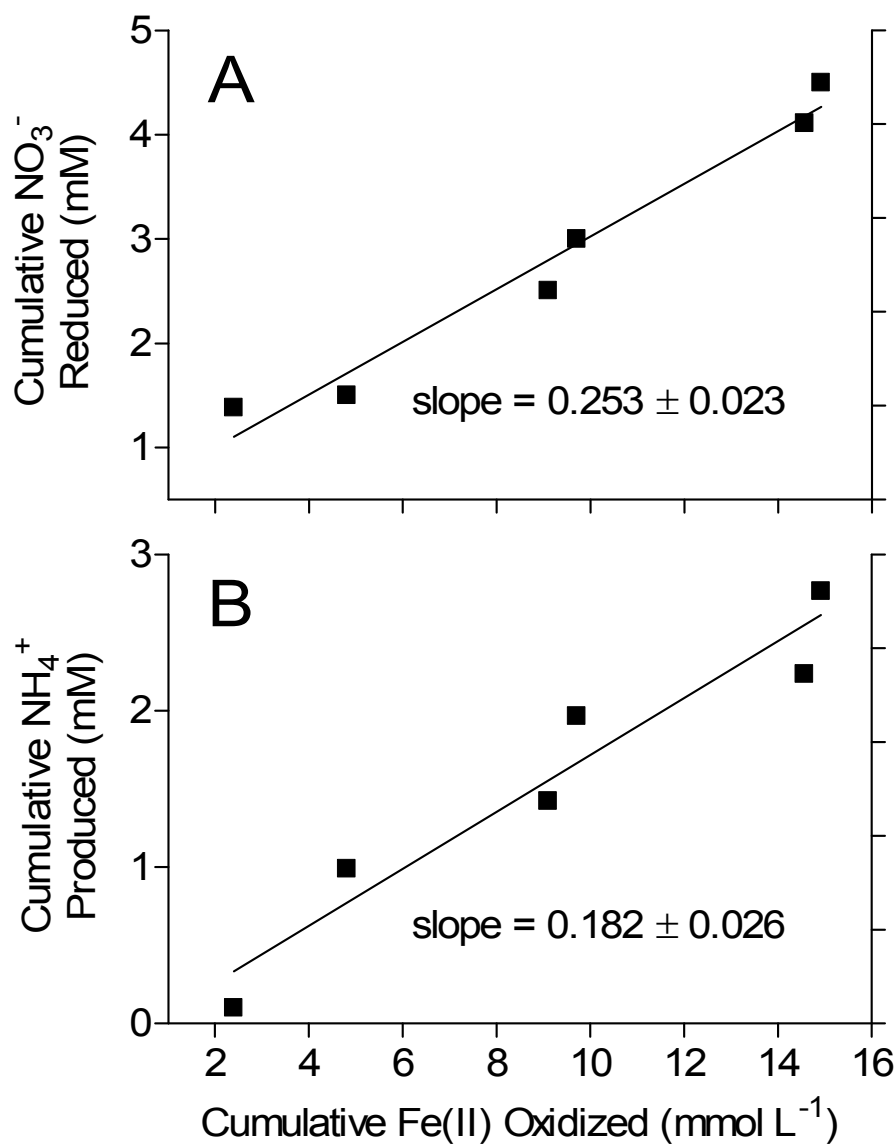


FIG. S2. Cumulative amount of nitrate reduced (A) or ammonium produced (B) versus the cumulative amount of Fe(II) oxidized during the last three periods of nitrate-dependent Fe(II) oxidation ($t > 50$ d) in the Fe cycling cultures. Data represent means of duplicate cultures.

Fig. S3

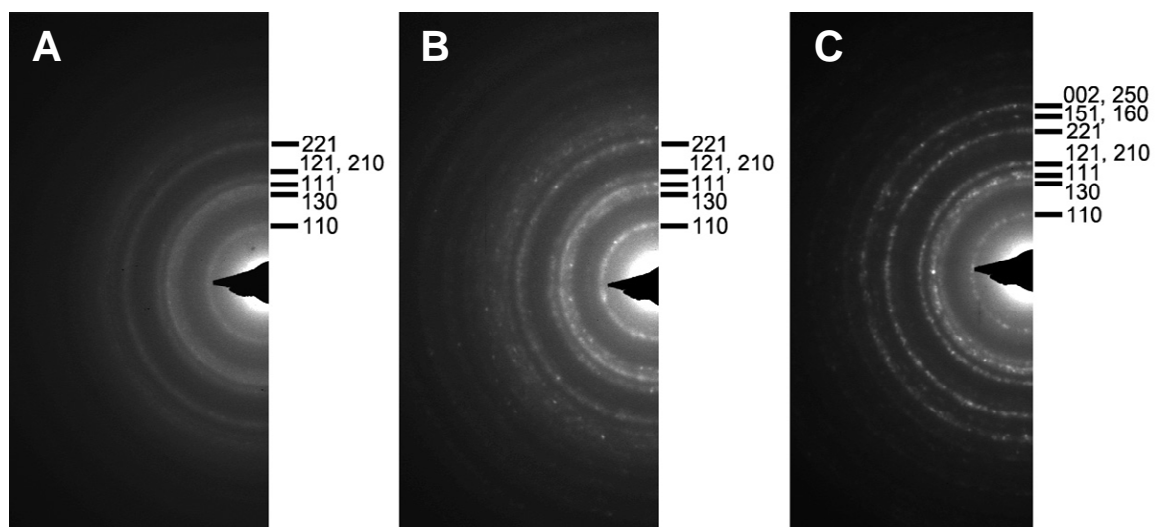


FIG. S3. Selected-area electron diffraction patterns for the high-resolution TEM images of samples from the nitrate-reducing (A), Fe(III)-reducing (B), and Fe redox cycling (C) cultures. The bright spots in panels B and C indicate an increase in the crystallinity of the oxide, although no evidence of new crystalline mineral phases is evident.